Trends in Analytical Chemistry 161 (2023) 117010

Contents lists available at ScienceDirect

Trends in Analytical Chemistry

journal homepage: www.elsevier.com/locate/trac

Mass spectrometry in materials synthesis

Jyotirmoy Ghosh, R. Graham Cooks*

Department of Chemistry, Purdue University, 560 Oval Drive, West Lafayette, IN, 47907, USA

ARTICLE INFO

Article history:
Received 6 December 2022
Received in revised form
14 February 2023
Accepted 28 February 2023
Available online 2 March 2023

Keywords:
Soft landing
Electrospray deposition
Microarrays
Nanomaterials
Preparative mass spectrometry

ABSTRACT

Mass spectrometry (MS), a century-old analytical technique, is now emerging as a preparative method. Electrospray deposition (ESD) of charged droplets generated by electrospray ionization (ESI) is an efficient means of forming nanomaterials, including catalysts. Much higher chemical specificity in the modification of surfaces can be achieved using mass-analyzed ions and performing ion soft landing (SL) although the low ion currents make this vacuum-based method slow. MS-based synthesis by either ESD or SL has considerable advantages over traditional approaches, providing control over the chemical identity, morphology, thickness, and surface patterning of materials while avoiding additives, ligands, and reducing agents. These MS-based methodologies are expected to provide considerable opportunities to optimize catalysts, prepare electronic devices or generate pure biopolymers.

1. Introduction

Mass spectrometry (MS) is a highly sensitive and specific analytical technique involving the formation, identification, and detection of ions. MS starts with the ionization of samples and proceeds via ion characterization using analyzers sensitive to mass-to-charge (m/z) ratios and then ion detection using sensitive particle detectors [1–3]. The discipline has repeatedly undergone revolutionary changes. One such was the development of the soft ionization methods, notably electrospray ionization (ESI) [4,5] and matrix-assisted laser desorption ionization (MALDI) [6], which enable the ionization of complex, nonvolatile, organic, or biological molecules. This capability led to the application of MS analysis in the emerging field of molecular nanoscience, e.g., determining the molecular formulas of noble metal clusters [7,8]. However, MS is much more than an analytical technique; given its basis in the manipulation of materials in ionic form, and is intrinsically a preparative method [9–21]. Preparative MS includes organic synthesis with the collection of macroscopic amounts of products, e.g., of ion/molecule reactions occurring in the gas-phase or in microdroplets, a topic that is not detailed here. This review instead focuses on materials preparation and surface modification, particularly on two types of experiments (i) those in which charged sprays of droplets are deposited on a surface in the ambient environment (ESD) and (ii) those in which isolated, mass-selected ions are deposited and/or reacted under vacuum (SL). In both types of experiments, materials are produced that are unavailable using conventional techniques.

An overview of the development and application of MS for the preparation of different kinds of materials is provided. The presentation starts with SL for materials synthesis using mass-selected ions under a vacuum. In the next section, ESD is presented, largely in connection with the synthesis of nanomaterials. The unique features of both experiment types include their freedom from counterions and additives, use of magnetron sputtering for synthesizing nanomaterials, and their surface patterning capabilities. In later sections, we discuss collector surface-driven nucleation mechanisms and the formation of monodispersed vs. polydispersed nanoparticles (NPs) by ESD. The penultimate section deals with different applications (catalytic, electrochemical, sensing) of the synthesized materials. In the final section perspectives for the future development of MS as a materials synthetic method are provided.

2. Soft landing

Ion soft landing is a process in which low-energy polyatomic ions (lab energies on the order of 10 eV) are deposited onto surfaces where they remain intact, viz. they do not lose their molecular connectivity upon landing [11,12,22–27]. At higher collision energies, dissociation (surface-induced dissociation) dominates while at lower energy ions are simply scattered from the surface [22]. Reactive collisions can occur with particular ion/surface combinations, with new bonds

* Corresponding author.
E-mail address: cooks@purdue.edu (R.G. Cooks).

https://doi.org/10.1016/j.trac.2023.117010
0165-9936/

being formed to the surface or in the deposited ion. In the first demonstration of the SL phenomena, small sulfur-containing ions were landed on metal surfaces [10], and subsequent work is reviewed in several articles [9,11,12,22–25,28–30]. The most distinctive feature of SL is the purity of the resulting materials, achieved because of the absence of counterions. The chemical nature of the ion, landing surface, and the collision energy altogether control the nature of any chemical bonding to the surface. Important phenomena associated with SL such as charge loss and ion desorption also influence the nature of the landed materials. Ion-neutralization is dominant for SL at a conductive surface [24], whereas retention of charge tends to occur at semi-conductive surfaces [26,31–33]. In the special case of matrices like self-assembled monolayers (SAMs) [26], charge can be preserved for hours or even days. Charge retention efficiency of soft-landed organic cations has been reported to decrease in the order of increasing hydrophilicity, fluorinated > alkyl > carboxylate-SAM surfaces. Retention of charge is more likely in multiply charged ions which give up their excess charges more readily than their last charge, as expected considering the relative recombination energies involved. Soft-landed cations can be neutralized via exothermic electron transfer across the interfaces or by loss of protons. Electron transfer from the anion to the surface is less thermodynamically favorable [34–36].

In a study on the details of charge transfer involving ions of different charge states (double, single, and neutral), Gramicidin S cations were soft-landed onto FSAM surfaces and their fate was analyzed by in situ Fourier transform ion cyclotron resonance mass spectrometry [34]. SL of the different charge states showed different time profiles, in which the abundance decreased for doubly charged and neutral species while it increased for the singly charged species. This result indicates a continuous deprotonation from the doubly charged species to form the singly charged ion, which is in agreement with the loss of protons being the major decay channels for polyatomic cations ions soft-landed on FSAM surfaces [24,34]. The rate constants for these processes suggest that proton loss is much faster than the desorption of ions from the surface [34]. In another study, [37] involving the SL of both $[Ni^{II}(salen)+H]^+$ and $V^{V}O(salen)^+$ complexes, [salen = N,N-ethylenebis-(salicylideneaminato) ligand] onto an FSAM surface, reduction of charge by proton loss from $[Ni^{II}(salen)+H]^+$ initiated an in situ redox reaction to form $V^{III}O(salen)^+$, a key intermediate in the four-electron reduction of O_2 [37] and indicative of the fascinating chemistry accessible by ion SL.

2.1. Soft landing in materials synthesis

SL has gained significant attention and found applications in the preparation of thin films [38,39]. Deposition of ionic clusters [40,41] of precise size and composition onto surfaces with well-defined coverage [21,42,43] allows tuning of catalytic properties by altering the size, composition, and surface coverage of the deposited clusters. SL provides the capability to deposit metal clusters with the desired numbers of atoms by employing mass-selection, and this controls their physical and chemical properties, specifically their catalytic properties [44,45]. In one such study, Heiz and co-workers [46] soft-landed mass-selected Ni cluster ions onto a MgO film. The soft-landed material was treated with CO, a model reaction in surface science, followed by examination of the reacting Ni clusters by infra-red (IR) and thermal desorption [46]. The experimental results suggested that the reactivity towards CO dissociation is $Ni_{30} > Ni_{20} > Ni_{11}$. Furthermore, the SL of the corresponding Pt_{15} cluster resulted in the catalytic oxidation of CO to CO_2 by activating adsorbed O_2 [47]. The high reactivity of the Pt_{15} cluster is mainly attributed to the optimum position of its electronic d-band which enables efficient back-donation of electrons and activation of adsorbed O_2. In another study [48], the catalytic activity of soft-landed small Au clusters (Au_x, $x < 20$) for the same oxidation was examined. The Au_8 cluster was found to be the smallest cluster that promotes oxidation [48]. Other than CO oxidation, many other reactions are promoted by soft-landed materials such as the reaction of CO with NO using Pd_{15} clusters [49], the oxidation of cyclohexane to CO and CO_2 using mass-selected Pd clusters [50], the epoxidation of propylene to propylene oxide by mass-selected Ag clusters [51], the epoxidation of propene by Au clusters [52], the polymerization of acetylene by Pd clusters [53], the oxidative dehydrogenation of cyclohexene by Co clusters [54], the decomposition of hydrazine by Ir clusters [55], and photocatalytic generation of H_2 gas by mass-selected Pt clusters on CdS nanorods [56].

SL has also been shown to be effective in creating useful electrode-electrolyte interfaces (EEIs) by depositing mass-selected electroactive ions onto electrodes [27,57,58]. EEIs are important for energy conversion and storage technologies [59]. SL of multielectron redox-active polyoxometalate (POM) anions ($[PMo_{12}O_{40}]^{3-}$) were utilized to study the effect of counterions on the performance of redox supercapacitors [57]. SL proved effective in eliminating the strongly coordinating counterions from POMs, and this resulted in a substantial decrease in the interfacial charge-transfer resistance and therefore enhanced performance of the POM-based redox supercapacitor [57]. SL and ESD showed contrasting outcomes in regard to the structures of the produced materials and contrasting performance as redox supercapacitors because SL allows mass-selective ion deposition, whereas ESD does not (Fig. 1a-b). Scanning transmission electron microscopy (STEM) images show uniformly distributed POM anions upon SL (Fig. 1c), whereas a substantial cation-POM aggregates on electrodes were observed in the case of ESD (Fig. 1d) [57]. This study shows that SL can be used to compare the redox properties of intact ions and their fragments, that enables rational design of EEIs. A similar study SL of mass-selected Ti nanoclusters (NCs) [58] showed a remarkable increase in the photoelectrochemical activity of metal oxide electrodes. SL also enabled controlled stoichiometry and of the distribution of electroactive species at EEIs [60].

2.2. Soft landing to create biomaterials

SL also has been instrumental in the synthesis of biomaterials. One example is the use of SL in the formation of protein microarrays on a surface [61]. In the earliest such study, protein microarrays were prepared by depositing selected charge states of cytochrome *c*, lysozyme, insulin, and apomyoglobin on an Au surface. Fig. 2a shows a photograph of the landed array of four different proteins in spots of 1 mm radius [61]. Fig. 2b shows an ESI mass spectrum of apomyoglobin after rinsing from the surface: the lack of any fragmentation indicates the intact deposition of the protein by SL on the surface while the wide distribution of charge states indicates collisional unfolding of the native conformation. It is interesting, however, that the biological activity of these simple hardy proteins is retained after SL, presumably because their refolding is facile [62,63].

In recent years, SL has begun to be applied to purify proteins and protein complexes for cryo-EM studies of their structures [64–68]. Cryo-EM is a stain-free imaging method that has the advantage of keeping the proteins hydrated at all times, so avoiding artifacts and aggregation [69]. Integration of cryo-EM with MS-based separation by ion SL creates a direct link between structural and chemical information obtained from cryo-EM imaging and MS [67]. In a different type of application, SL has been utilized for the chiral enrichment of mass-selected protonated serine octamers [70], enrichment being confirmed by redissolution of the landed

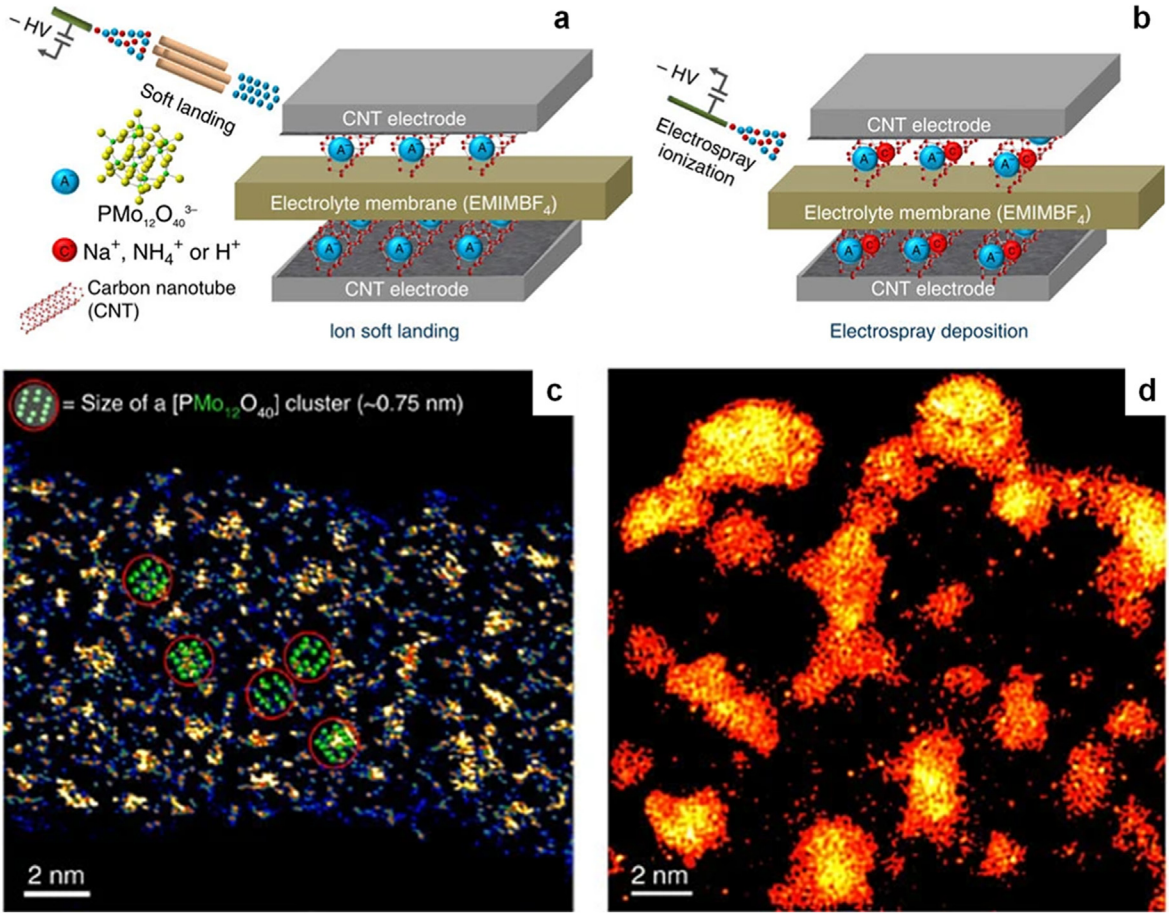

Fig. 1. Schematic representation of electrode-electrolyte interfaces (EEIs) of redox-supercapacitors fabricated by **(a)** SL and **(b)** ESD of $[PMo_{12}O_{40}]^{3-}$ onto CNT electrodes. High-resolution STEM images of the POMs formed on the electrode by **(c)** SL and **(d)** ESD. Reprinted from Ref. [57] with permission from Nature Publishing Group.

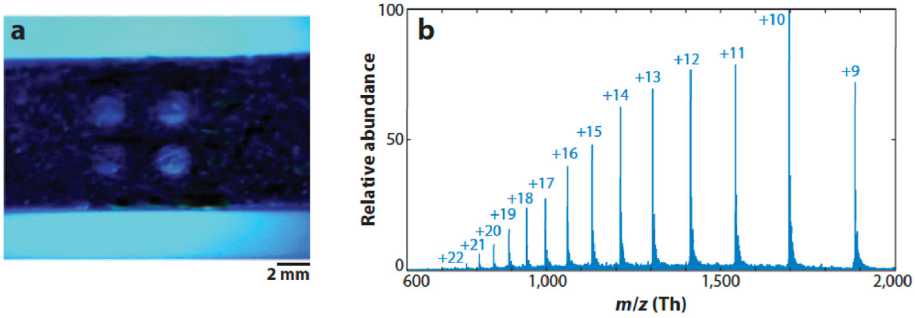

Fig. 2. (**a**) Photograph of soft-landed microarray of four proteins onto Au substrate, where each spot is having a radius of 1 mm. (**b**) ESI mass spectrum generated by rinsing the soft-landed apomyoglobin spot. Reprinted from Ref. [61] with permission from American Association for the Advancement of Science.

material and comparison of the pre- and post-landing pattern of MS intensities using optical isomer selective isotopic labeling [70]. In another study [71], 2D chiral amplification was achieved by SL of trioctyl-functionalized triazatriangulenium ions on Au(111) and Ag(111) surfaces in ultrahigh vacuum (UHV). The three octyl chains attached to the molecular core are bent due to steric and surface interactions and therefore the molecule is adsorbed on the surface in the gauche form. Only one of the eight possible configurations of the octyl groups was observed in STM images. SL led to chiral amplification in the hexagonal islands of the deposited molecular networks [71].

MS allows the precise control of the ion beam in terms of chemical entity, charge state, and kinetic energy and it therefore allows controlled preparation of protein or peptide films. Fig. 3a shows a schematic representation of both ESD and SL of $AcA_{15}K$ peptide ions on SAM surfaces [72]. Infrared reflection-absorption spectra (IRRAS) were recorded from the surface upon ESD and SL and they suggested the formation of a β-sheet-dominated peptide layer by ESD and an α-helical peptide layer by SL (Fig. 3b) [72]. Molecular dynamics (MD) simulations showed a stable α-helical conformation of $AcA_{15}K$ peptide in the gas phase. This conformation was stabilized by the interaction between the protonated C-

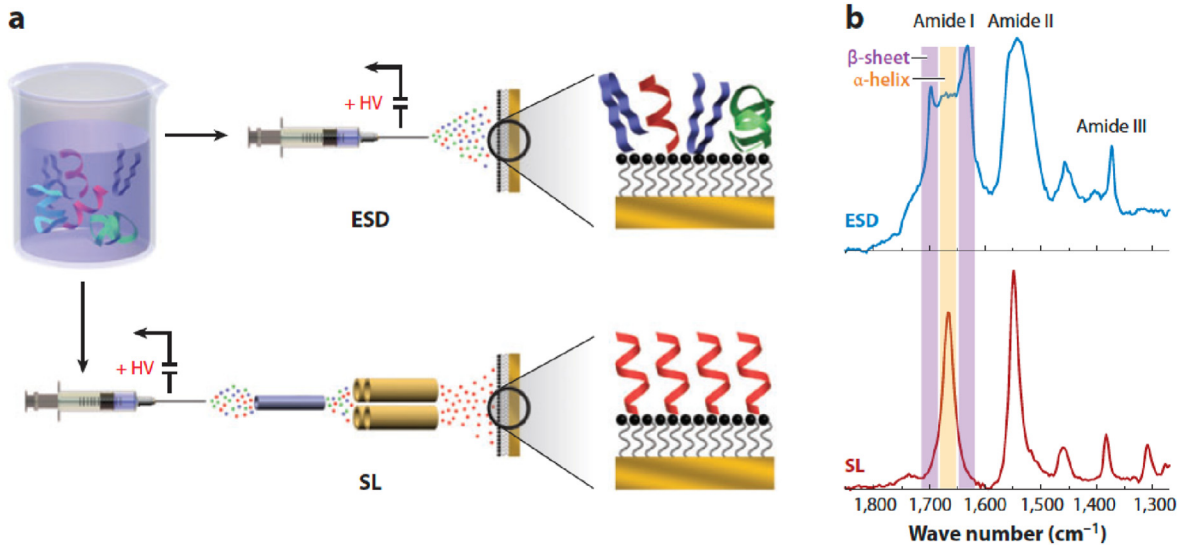

Fig. 3. **(a)** Schematic representation of electrospray deposition (ESD) and soft landing (SL) of peptide ions onto self-assembled monolayer (SAM) surface. **(b)** Infrared reflection-absorption spectra (IRRAS) of $AcA_{15}K$ peptide layer onto SAM surface created by (top) ESD and (bottom) SL, respectively. The features at 1632 and 1697 cm^{-1} are the characteristic features of β-sheets, and observed in the case of ESD, whereas the sharp feature at 1670 cm^{-1} is characteristic of α-helical conformations as generated by ion SL. Adapted from Ref. [72] and Ref. [23] with permission from Wiley and Annual Review.

terminal lysine residue and the dipole of the helix [73–76]. SL resulted in this α-helical conformation being retained in the ambient environment for at least 20 days [72]. The formation of the β-sheet in the case of ESD is not completely understood but it was suggested that ESD retained the β-sheet dominated structure found in the solution phase [72]. This study demonstrated that the SL of mass-selected peptide ions can be used for the preparation of conformation-specific peptide arrays on SAM surfaces [72].

Electrospray ion beam deposition (in this review, we use the original term SL) of biological molecules, specifically proteins, allows control over their conformation [10,19,26,77,78], and so dictates the physical and chemical properties of the deposited proteins. The 3D structural characterization of proteins with spatial resolution at the atomic level is achievable by the combination of SL with surface-sensitive scanning tunneling microscopy (STM), which characterizes the individual landed proteins [9]. While MS allows the identification of proteins in terms of peptide sequences, STM characterizes the protein conformational structure in space and both methods (indirectly or directly) achieve atomic precision. To demonstrate the power of this combined approach, ion beams of the protein CytC were deposited on a flat metal surface followed by STM imaging. The entire workflow is shown in Fig. 4a [79]. The conformational states of CytC (folded or unfolded) are directly related to the charge state of the landed protein ions. Many protein studies suggest that the higher charge state ions ($z > +10$) correspond to the unfolded structures, while lower charge state ions ($z < +8$) arise from folded and partially unfolded proteins [80]. Therefore, the selection of the m/z range of the desired high- or low-charge states directly reflects the conformational structure in the STM micrographs. Fig. 4b shows the STM images of the selected charge states of CytC ion beams soft-landed onto the Cu(100) surface UHV [80]. Fig. 4b shows lower charge states from $z = +3$ to $+8$, correspond to mostly globular-like folded or native CytC proteins [81–83]. As the charge state was gradually decreased, the protein conformations were also found to be different ranging from extended, almost straight strands ($z = 17–19$), to more curved strands ($z = 14$, 15, and $z = 12$, 13), to compact two-dimensional patch ($z = 12$, 13 and $z = 8$, 9). The STM images of the unfolded and folded proteins are distinct, folded proteins appear as globular, whereas unfolded proteins appear as extended strands. In this case, the interaction between the protein chains and Cu(100) surface was quite strong which always led to 2D structures, and the 3D structure only formed due to deposition of the native conformation of the protein [80].

3. Electrospray deposition in synthesis of nanomaterials

ESD was first introduced as a fabrication tool to prepare thin radioactive materials used in nuclear research [84–88]. Subsequently, it was utilized in various areas such as for the modification of silicon surfaces [89], semi-conductive ceramics [90], polymer coatings [91], DNA and protein films preparation [92], biologically active protein deposition [93–95], and nanomaterials synthesis [96]. This method has provided sufficient versatility to prepare a variety of structures without use of hazardous oxidants or reductants. There are several studies that deal with the fundamental aspects of electrospray in the context of materials synthesis [97–99]. While ESD is not strictly an MS method, ESI is the most common MS ionization method and MS is often used to characterize the materials that result from ESD.

ESD under ambient conditions has emerged recently as a new method for a range of nanomaterials. The experiment does not have the advantage of deposition of mass-selected species nor is it solvent free, but the chemical nature of the solvated ions contained in ESD-charged droplets is usually known. The solvated ions are reduced to form nanostructures when the droplets making up a dispersed plume collide with an electrically grounded surface. Depending on the nature of ions in microdroplets and collecting surfaces, ESD can result in several forms of materials. Examples include the synthesis of NPs [100,101], nanobrushes [102], nanowires [103,104], nanoclusters [105,106], nanoplatelets or nanopyramids [107], nanosheets [108,109], monodispersed NPs [110], nanosized onion-like carbon (OLC) [111], etc. The choices of collecting surfaces include flat metal surfaces [107], ITO plates [110,111], water [109], MoS_2 nanosheets [108], Te nanowire [112], TEM grids [102], etc.

Electrochemical corrosion-based ion generation from coinage metals (Ag, Au, and Cu) and its deposition to synthesize NPs was

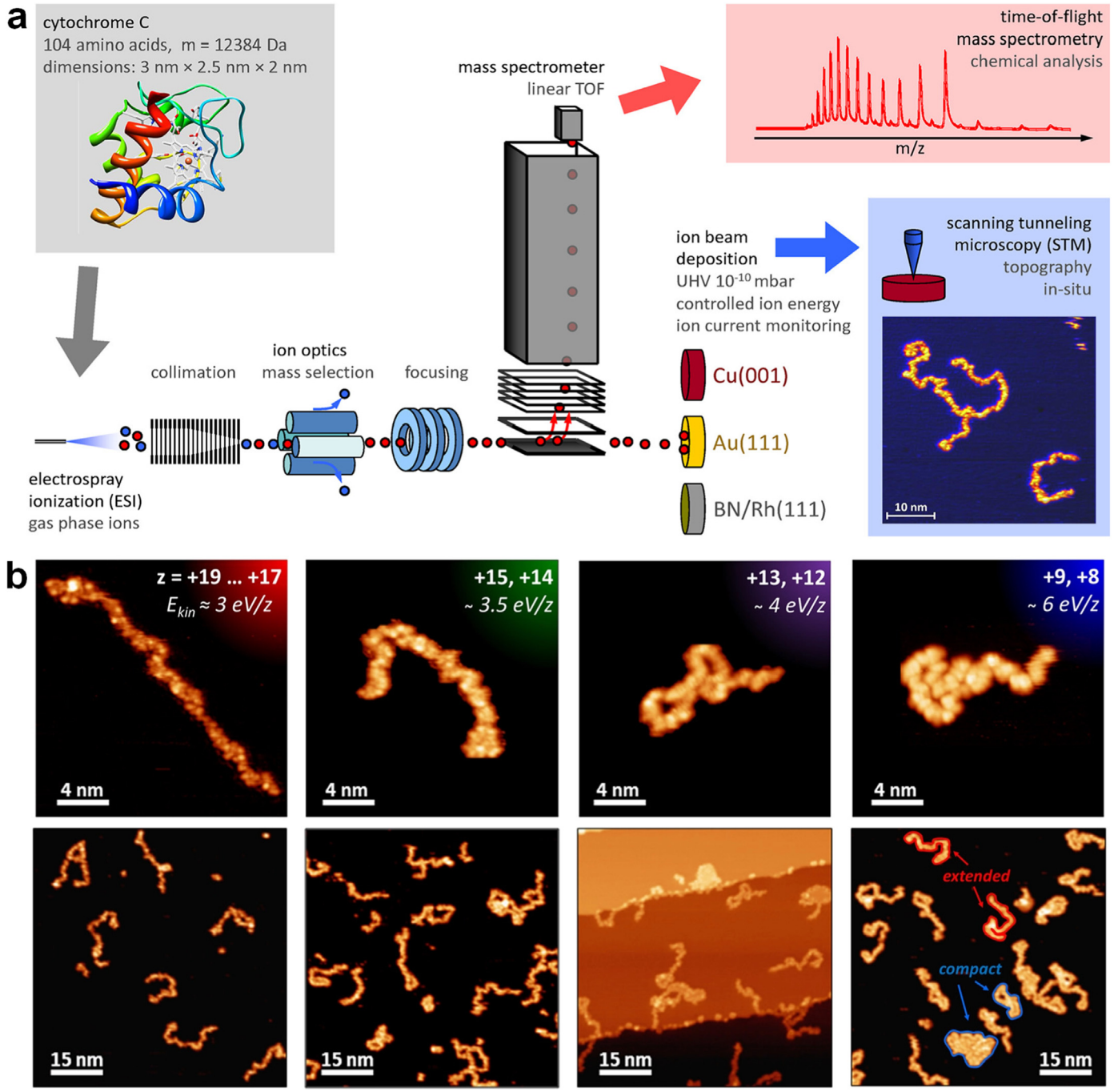

Fig. 4. **(a)** Schematic representation of SL of CytC protein. After the ionization of protein by ESI, the protein ions are collimated, mass-selected, and focused by the ion optics assembly. The ion beam is deposited onto different flat metal surfaces in ultrahigh vacuum (UHV). TOF-MS and STM are used to analyze the chemical composition and topography of the landed proteins, respectively. Reprinted from Ref. [79] with permission from American Chemical Society. **(b)** STM images of filtered CytC ions of different charge states deposited onto the Cu(100) surface in UHV. Reprinted from Ref. [80] with permission from American Chemical Society.

first introduced in 2014 [100]. Fig. 5a shows the presence of Ag-containing ions in the mass spectrum when anhydrous acetonitrile was electrosprayed from the Ag electrode-based nano-electrospray emitter. Electrocorrosion of Ag occurred with anhydrous acetonitrile but not when spraying MeOH/H_2O solvent. Direct deposition of these charged droplets on a grounded surface like a TEM grid led to neutralization and aggregation to form metal NPs. Fig. 5b and c show TEM images of the Au NPs electro-deposited onto TEM grids at different scales. The Au NPs synthesized by this method were utilized as a catalyst for the $NaBH_4$-assisted reduction of *p*-nitrophenol [100]. Fig. 5d shows the UV–vis spectra for the reduction of p-nitrophenol by directly electrospraying Au ions onto the surface of the grounded reaction mixture. This electrodeposition method was also used for the synthesis of Cu NPs, which act as catalysts for the polymerization of styrene [100]. In another study [102], an aqueous solution of AgOAc was electrosprayed onto a TEM grid, which led to the brush-like growth of nanowires, as shown in Fig. 5e–h. The corresponding ESI mass spectrum shows the presence of Ag and hydrated Ag ions. Lee et al. [103] demonstrated that Au NPs and their self-assembly led to the spontaneous formation of

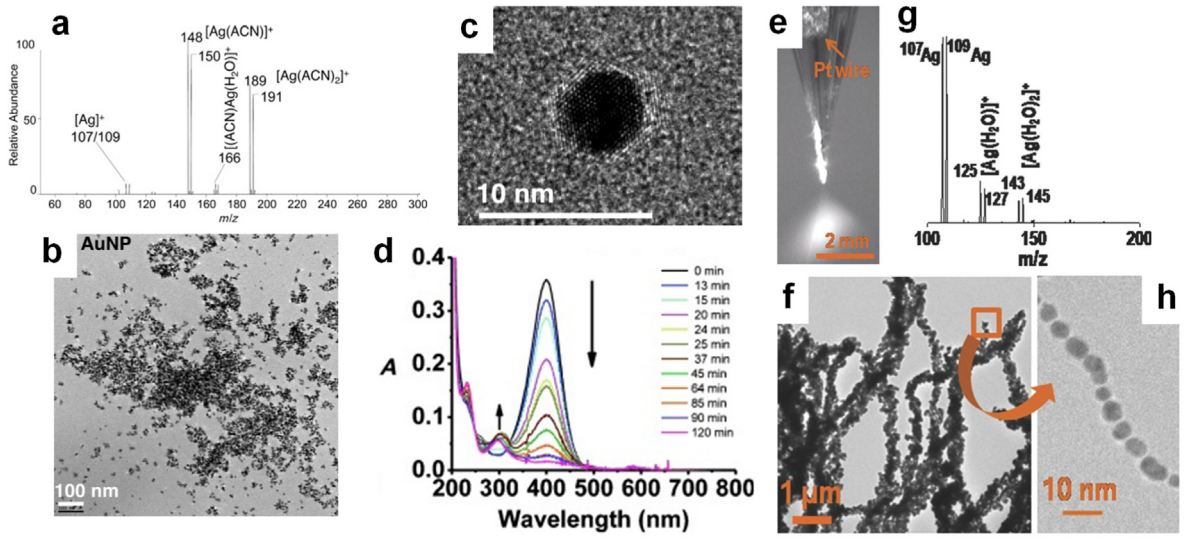

Fig. 5. **(a)** Nano-ESI mass spectrum generated by electrospraying acetonitrile (ACN) from a nanoelectrospray emitter holding an Ag wire electrode. Au nanoparticles (NPs) synthesized by electrocorrosion of Au wire electrode and their **(b)** TEM and **(c)** high-resolution TEM image. **(d)** UV–vis spectra for the reduction of p-nitrophenol with online added charged droplets containing Au^+ ions, which formed AuNPs and subsequently catalyzed the reduction. Reprinted from Ref. [100] with permission from Wiley. **(e)** Photograph of electrospray of aqueous solution of AgOAc. **(f)** Mass spectrum generated from the electrospray of AgOAc solution. **(g)** TEM and **(h)** high-resolution TEM image of Ag nanobrush. Reprinted from Ref. [102] with permission from Wiley.

Au nanowires by fusing microdroplets on a microsecond time scale at ambient conditions. The rate of formation for these nanostructures was several orders of magnitude greater than in bulk solution. The air-water interface of microdroplets provides localization or self-alignment of reactants at the surface as well as a strong electric field, which enables the accelerated synthesis of nanostructures [103,113–115].

3.1. Ligand-free electrospray deposition (ESD)

Conventional methods of nanomaterials synthesis often require a stabilizing ligand, which needs to be removed before utilization of the product in studies like electrocatalysis [116,117]. However, ESD can be used to synthesize nanomaterials without stabilizing ligands [116,118–120]. Two different types of electrodeposition methods can be used to synthesize ligand-free nanomaterials, (a) the electrospray-based deposition of solvated metals ions [100,102,109,121,122], and (b) electrochemical deposition of droplet-mediated metal ions at an ultramicroelectrode surface [116,118–120]. The latter method provides more control over the size, morphology, roughness, and coverage of metal nanomaterials [118]. Briefly, this method utilizes water droplets containing the metal as its precursor salt in the ionic form, suspended in dichloroethane (DCE). Sonication is applied to create droplets of ~500 nm radius which then collide with the electrode forming the metal NPs [116,118–120].

3.2. Synthesis of nanoclusters (NCs)

He et al. [97] has suggested that ESD-generated materials can be classified based on their shapes such as spherical, non-spherical, and assembled structures. ESD has been used to form spherical (NPs) as well as non-spherical structures, such as NCs [105,106], nanoplatelets or nanopyramids [107], and nanosheets, [108,109]. Atomically precise metal NCs have emerged as very important materials in terms of energy storage, catalysis, photoluminescence, sensing, and some biological applications [7,123–126]. NCs are structurally different from NPs and they behave more like molecules [7]. A classic example is fullerene, C_{60}, the widely known stable carbon cluster that was first discovered using mass spectrometry [127] by focusing a pulsed high-powered laser and vaporing solid graphite. The resulting vapors were cooled in a high-density helium stream, which led to the formation of carbon clusters, that were detected and characterized by time-of-flight (TOF) MS. Fig. 6 shows the TOF mass spectra of carbon clusters at different flow densities of helium gas, where the major constituents are C_{60} and C_{70} cluster [127]. In Fig. 6c, a gaussian distribution of large and even-numbered clusters with 38–120 carbon atoms was observed in the presence of a low-density helium stream. As the pressure was increased to ~760 torr, the intensity of the C_{60} peak increased (Fig. 6b), and adding an integration cup for the delayed expansion of the vapor led to prominent features corresponding to C_{60} and C_{70} clusters in the mass spectrum (Fig. 6a) [127]. Recently, ESD was utilized to synthesize protein-protected Au (Au@BSA, Au@Lyz; BSA = bovine serum albumin and Lyz = lysozyme protein) and Ag NCs (Ag@BSA) as shown in Fig. 6d [105]. The TEM image of Au@BSA reveals the average diameter of the NCs is 1.5 nm (Fig. 6e). Furthermore, MALDI MS was utilized to confirm the Au@BSA cluster and the difference in mass between BSA and Au@BSA cluster peak indicates that the cluster comprises 30 Au atoms (Fig. 6f). The rate of formation of this "molecular material" utilizing microdroplet-based synthesis was greatly enhanced as compared to the traditional synthetic approach [123,124,126]. Further, it was demonstrated that these NCs with biological ligands such as proteins (BSA, lysozyme) retain their biocompatibility and that their luminescence can be utilized for in vitro imaging, e.g., of retinoblastoma cells [105]. This unique and simple method of nanomaterial fabrication also resulted in the formation of different phases of Cu sulfide nanostructures [107]. These findings indicate that the synthesis of nanomaterials by ESD is very efficient and that it does not require multiple steps, long reaction times, high temperatures, or the use of additives as required in conventional synthetic approaches.

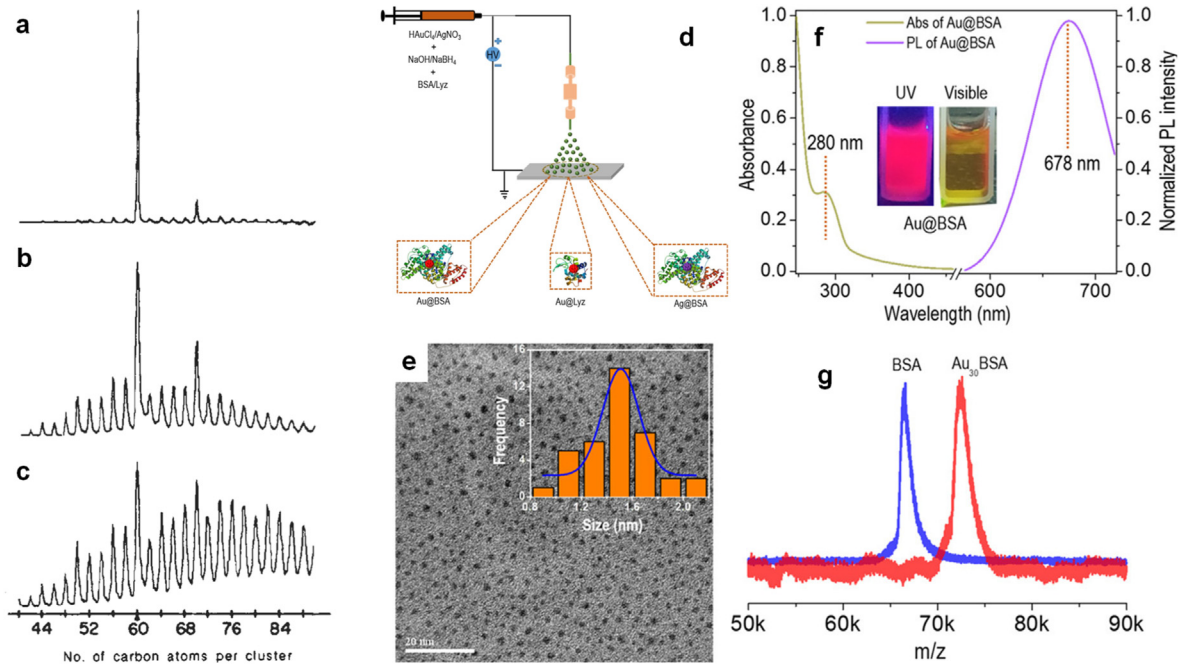

Fig. 6. Mass spectra of carbon clusters generated by laser vaporization of graphite and subsequent cooling in a helium stream of **(a)** 760 torr in the integration cup, **(b)** 760 torr, and **(c)** 10 torr. Reprinted from Ref. [127] with permission from American Association for the Advancement of Science. **(d)** Schematic representation of ESD setup for the synthesis of Au@BSA nanocluster, where BSA = bovine serum albumin protein used as protecting ligand. **(e)** TEM image, **(f)** UV–vis spectrum (left) and photoluminescence (PL) spectrum (right), **(g)** MALDI MS spectra of Au@BSA cluster synthesized by ESD. Reprinted from Ref. [105] with permission from American Chemical Society.

3.3. Surface patterning

The micropatterning of surfaces is important in the fields of optics, biotechnology, and electronics. Different techniques such as photolithography, soft lithography, and ink jetting have been widely used for microfabrication, however, they have limitations in terms of accessing surfaces with an inherent variety of chemical and physical properties, as well as high cost and inconvenient and complex procedures [128,129]. Deposition of ion beams onto surfaces by both ESD and SL is emerging as an effective method for patterning on surfaces [61,112,121,130–132]. In addition, MS enables surface modification with specific analytes by mass-selection or selective reactivity e.g. transhalogenation at the surface [133,134] and it also provides control over the incident ion energy range. It is simple to control the shape and size of the landed spots by changing the beam direction and the shape of the aperture through which the ion beam passes [132]. The size of the patterned spots also depends on the voltage supplied to the collection electrode [132]. Representative studies include trialkyl silyl cation (SiR_3^+) patterning on OH-terminated SAM surfaces [130,131], SL of mass-selected protein ions to create mm-size microarrays [61], ESD of Ag ions using electrically floated masks to focus the ion beams to create a patterned surface with Ag NPs spots with 20 μm diameter [121]. These NPs spots showed surface-enhanced Raman spectroscopy (SERS) activity [121]. In another study [135], a low-energy platinum nanocluster beam produced by laser vaporization was deposited onto HOPG surfaces, which led to the self-organization of NCs into dense arrays.

3.4. Magnetron sputtering in synthesis of nanoclusters (NCs)

Apart from SL and ESD which are the most widely used materials synthetic methods involving ions, magnetron sputtering has emerged as an alternative technique to produce charged clusters for the synthesis of solid materials of different size and composition, including those that could not be generated by solution phase synthesis [136]. This method has advantages as a nonthermal method capable of producing continuous beams of large fluxes of mass-selected ions. High-power impulse magnetron sputtering (HiPIMS) coupled with a gas flow cell reactor was utilized to synthesize Ag_n^- NCs ($n = 1–73$) [137]. Time-resolved mass spectrometry was utilized to understand the growth mechanism of these NCs by gradually increasing ion flux using higher peak powers and repetition rates of the HiPIMS [137]. Various NCs were effectively generated by magnetron sputtering. They included clusters of different sizes and compositions such as $TaSi_n$ [138], small-sized metal clusters encapsulated in silicon cages, $M@Si_{16}$ (M = Ti, V, Nb, and Ta) [139–143], charge transfer complexes, $(Ta@Si_{16})^+C_{60}^-$ [144], Ag_n or Au_n NCs [145–147], ligand-free Pt NCs supported on Marimo carbon powder [148], mass-selected negatively charged $Mo_{100\pm2.5}$ and $(MoO_3)_{67\pm1.5}$ clusters [149], ligand-free Mo_n^- clusters of different core sizes [150], $(TiN)_{141}$ clusters [151], $PtZr_2O_7$ clusters supported on HOPG for catalytic dehydrogenation of 1-propanamine [152], size-selected $(ZrO_2)_3$ for decomposition of dimethyl methylphosphonate, a chemical warfare agent [153] $(WO_3)_n$ and $(MoO_3)_n$ ($n = 1, 2, 3, 5, 30$) for catalytic dehydration of 2-propanol [154], $(WO_3)^{3-}$ clusters [155], the $(PbS)_{32}$ cluster [156], and Mo_n^-, W_n^-, and Fe_n^- cluster anions [157].

Further, magnetron sputtering was utilized to synthesize model catalysts such as elemental Pd, and binary PdSn and PdTi clusters for the selective hydrogenation of 1-pentyne and 3-hexyn-1-ol [158]. This method offers several advantages such as the fact that the clusters need not have ligands, mass-selected ions provides precise size determination and control, and clusters of various combinations of metals can be readily produced [158]. Using a customized multi-target magnetron sputtering/gas aggregation source, Laskin and co-workers synthesized bare PtRu NPs, which catalyzes electrochemical reduction of oxygen [159], size-selected PtTi alloy NPs [160], and bare Pt_{30} NCs for oxygen reduction reaction [60].

4. Physical phenomena

4.1. Selection of collector surface

The type of collector surface during ESD also dictates the nucleation mechanism and morphology of the deposited materials. ESD of metal ions deposited on a flat surface tends to lead to the formation of NPs [100,121], whereas changing the surface to an uncoated TEM grid results in 3D growth of nanobrush morphology [102]. TEM images revealed that the morphology of Ag nanowires formed this way is made up of "pearl necklace" like rows of individual Ag NPs, as shown in Fig. 5h. The enhanced electric field at the nanowire tip causes the growth of 1D nanowires [102]. Further, ESD of Pd ions onto the surface of water resulted in NPs that further self-organize to form Pd nanosheets induced by electrohydrodynamic flow, under the influence of the electric field induced by the applied potential [109]. Further, experimental results suggest that nanosheet formation by ESD is independent of the type of metal and liquid surface chosen, therefore a strong underlying physical phenomenon must be at play. The authors [109] suggested that ESD creates a strongly charged electrical double layer at the liquid-air interface [161]. The tangential electric field at the interface creates a steady flow, which guides NPs to assemble into nanosheet structures. The type of collector surface also influences the dimensionality of the resulting nanostructures such as 1D Ag nanowires [102], 2D Pd nanosheets [109], and 3D Cu_xS nanopyramids [107] were formed by ESD onto TEM grid, water surface, and flat solid Cu surface, respectively.

4.2. Monodispersed materials

ESD has also emerged as a medium for the fast and facile transformation of polydispersed NPs to their monodispersed analogs. Usually, these processes require post-synthetic treatments, digestive ripening, and refluxing, and they are quite slow [162–165]. In a recent study [110], ESD was used to convert thiol-protected polydispersed Ag NPs of 15 ± 10 nm diameter to monodispersed Ag NPs of 4.0 ± 0.5 nm diameter (Fig. 7). This phenomenon is extremely fast (in the order of seconds) and it occurred without added chemicals, templates, or high temperatures. The authors have suggested that microdroplet experiences annealing during electrospray which is analogous to the digestive ripening but on a microscale and this changes the dispersity of the NPs [110]. In another study, when polydispersed solutions of diphosphine-capped Au clusters were electrosprayed and deposited onto carbon-coated Cu grids, they resulted in monodispersed Au_{11} clusters as confirmed by TEM analysis [166]. However, in a contrary study, ESD is shown to transform nanodiamonds (11 ± 1 nm in size) into onion-like carbons (50 ± 13 nm in size) [111]. A high voltage was essential for this last transformation [111].

5. Applications

Materials fabricated by ion deposition have been utilized for many applications such as catalyzing organic reactions [100,101,109], catalytic polymerization [100,102], surface-enhanced Raman spectroscopy (SERS) [121], electrochemical reduction of oxygen [159,167], electrochemical water splitting [168], in vitro imaging within a biological system [105], disinfection of water [108], and atmospheric water capture [104].

5.1. Catalytic applications

The utilization of Ag nanocatalysts for the reduction of *p*-nitrophenol has already been discussed (Fig. 5d). Related examples include fabrication by ESI of an AgPd nanobrush that showed catalytic activity for the polymerization of diphenylamine (DPA) with a conversion efficiency of 58% [102], whereas in another study [100], Cu NPs created by ESD acted as a catalyst for radical polymerization of styrene. Moreover, Pd nanosheets generated by ESD were utilized as a catalyst for the Suzuki-Miyaura coupling reaction between aromatic boronic acid and an organohalide [109]. The catalytic efficiency of this nanosheet was found to be ~23 times higher than a common commercially available catalyst, tetrakis(-triphenylphosphine) palladium(0) [109]. In a recent click chemistry study [101], it was demonstrated that ESD of Cu ions onto the surface of an acetonitrile solution of an azide-alkyne cycloaddition (AAC) click reaction mixture led to the formation of a film of heterogeneous catalyst comprised of small-sized Cu NCs. This NC-catalyzed the AAC click reaction between a terminal alkyne and organic azide to synthesize, regioselectively, 1,2,3-triazoles. Experimental results suggest that diffusional mixing leads to physical contact between the catalyst and the reactants plays an important role in the reaction kinetics [101].

5.2. Electrochemical applications

SL of mass-selected ions was utilized to create bimetallic PtRu NPs of 4.5 nm diameter on glassy carbon electrodes [159]. This nanomaterial was uniform in size and morphology as observed in high-angle annular dark field mode scanning transmission electron microscopy images and used for the electrochemical reduction of oxygen as evaluated by cyclic voltammetry [159]. Further, reactive magnetron sputtering resulted in Ta ions which were soft-landed along with 2-butanol, heptane, and m-xylene, individually and it led to the fabrication of organic-inorganic hybrid NPs [167]. The Ta-heptane and Ta-xylene NPs were found to be catalytically active toward oxygen reduction, whereas the pure Ta and Ta-butanol NPs were unreactive [167]. Electrosprayed charged droplets were utilized to fabricate NiFeOOH with rich oxygen vacancies at the interface between charged droplets and Ni foam. This material demonstrated electrocatalysis in water splitting [168].

5.3. Other applications

Patterned Ag NPs formed by ESD are useful in creating SERS active surfaces and in tuning their plasmon resonance properties [121]. These nanostructured patterned spots showed an average SERS enhancement factor of 10^8 when created using different lasers (532, 633, and 785 nm) [121]. ESD-generated Au@BSA cluster showed enhanced luminescence and this property was utilized for sensing in a biological system, more precisely for in vitro imaging of retinoblastoma NCC-RbC-51 cells [105]. ESD was also utilized to create holey MoS_2 nanosheets, where Ag ions were deposited on MoS_2 nanosheets suspended in water. The Ag ions reacted with S of the nanosheets creating Mo-rich holes of 3-5 nm. These Mo-rich defects in the nanosheet generated active oxygen species (H_2O_2), which caused effective disinfection of water from different bacterial and viral strains [108]. Another application of Ag nanowire assemblies (nanobrush) formed by ESD was to capture bacteria and particulate matter [102]. Utilizing this capturing property, hydrophilic-hydrophobic patterned nanowires were synthesized, which showed atmospheric water capture (AWC) capability [104]. The concept of AWC by these nanowires was inspired by similar phenomena observed in cacti and Namibian Desert beetles.

6. Conclusion

We have discussed the recent developments of MS as a materials synthetic tool. The discussion highlights the fabrication of

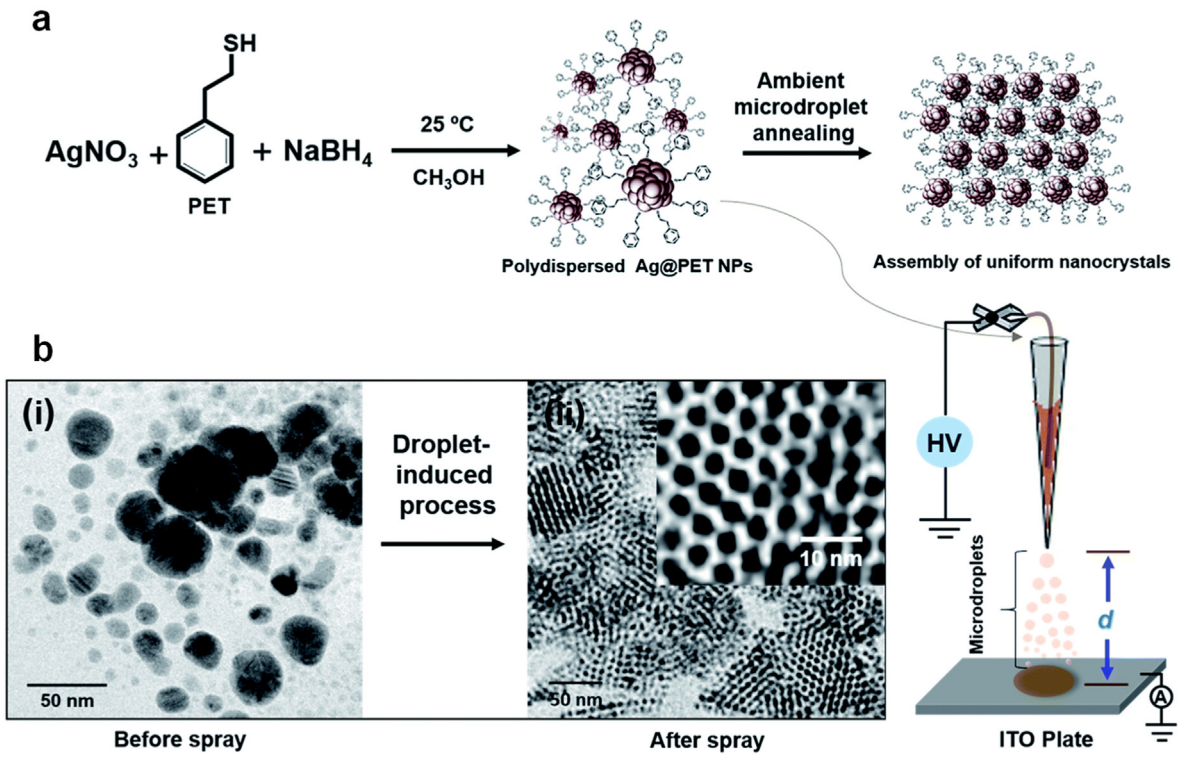

Fig. 7. **(a)** Schematic of the synthetic steps of polydisperse Ag@PET nanoparticles (NPs) and its conversion to monodisperse analogs by ambient microdroplet annealing. Schematic of the experimental set-up for ESD of Ag@PET NPs on an ITO (indium tin oxide) plate **(b)** TEM images of Ag@PET NPs before and after ESD on an ITO plate. Reprinted from Ref. [110] with permission from The Royal Society of Chemistry.

materials by SL and ESD. The deposition of mass-selected species by SL results in the controlled synthesis of high-purity inorganic and biomaterials and examples of their utilizations have been discussed. On the other hand, ESD is a relatively simple and ambient technique, which is utilized to synthesize different nanomaterials, and the associated physical phenomena have been discussed. The utilization of these materials in many practical applications is intriguing. It is noteworthy that the simplicity of creating catalysts by deposition of ions suggests a catalyst-on-demand capability. Moreover, combining this simple synthetic method with high throughput reaction screening capabilities such as those provided by DESI-MS [169,170] creates new methods of examining large numbers of catalysts and optimizing their performance. This is a new frontier in catalyst science [171].

The fabrication of the important materials discussed here on a reasonable scale by SL methods is limited by the low mass-selected ion currents available by MS. On the other hand, ESD can be performed with multiple spray sources generating high material fluxes [172]. As a future direction, high-transmission bright ESI ion sources in multiplexed format should answer this challenge. Accelerated synthesis of materials by electrosprayed microdroplets while screening their properties in a high-throughput format would be another direction to move forward. Finally, all these aspects make the MS-based synthesis of materials important, unique, challenging, and attractive, and many new studies in this area in the future will enhance the scope of this subject.

Declaration of competing interest

The authors declare that they have no known competing financial interests or personal relationships that could have appeared to influence the work reported in this paper.

Data availability

Data will be made available on request.

Acknowledgments

We acknowledge financial support from the National Science Foundation (NSF), grant number CHE-1905087, and from the Multi-University Research Initiative (MURI) of the Air Force Office of Scientific Research (FA9550-21-1-0170) via Stanford University (sub-award 62741613-204669). The authors thank Mr. Hugo Yuset Samayoa Oviedo and Dr. Depanjan Sarkar for helpful comments.

References

[1] F.W. McLafferty, A century of progress in molecular mass spectrometry, Annu. Rev. Anal. Chem. 4 (2011) 1–22.
[2] R.S. Gohlke, F.W. McLafferty, Early gas chromatography/mass spectrometry, J. Am. Soc. Mass Spectrom. 4 (1993) 367–371.
[3] R.W. Kondrat, R.G. Cooks, Direct analysis of mixtures by mass spectrometry, Anal. Chem. 50 (1978) 81A–92A.
[4] J.B. Fenn, M. Mann, C.K. Meng, S.F. Wong, C.M. Whitehouse, Electrospray ionization for mass spectrometry of large biomolecules, Science 246 (1989) 64–71.
[5] J.B. Fenn, M. Mann, C.K. Meng, S.F. Wong, C.M. Whitehouse, Electrospray ionization–principles and practice, Mass Spectrom. Rev. 9 (1990) 37–70.
[6] Michael Karas, Doris Bachmann, Franz Hillenkamp, Influence of the wavelength in high-irradiance ultraviolet laser desorption mass spectrometry of organic molecules, Anal. Chem. 57 (1985) 2935–2939.
[7] I. Chakraborty, T. Pradeep, Atomically precise clusters of noble metals: emerging link between atoms and nanoparticles, Chem. Rev. 117 (2017) 8208–8271.
[8] C.A. Fields-Zinna, R. Sardar, C.A. Beasley, R.W. Murray, Electrospray ionization mass spectrometry of intrinsically cationized nanoparticles, $[Au_{144/146}(SC_{11}H_{22}N(CH_2CH_3)_3^+)_x(S(CH_2)_5CH_3)_y]^{x+}$, J. Am. Chem. Soc. 131 (2009) 16266–16271.
[9] S. Rauschenbach, M. Ternes, L. Harnau, K. Kern, Mass spectrometry as a

preparative tool for the surface science of large molecules, Annu. Rev. Anal. Chem. 9 (2016) 473–498.
[10] V. Franchetti, B.H. Solka, W.E. Baitinger, J.W. Amy, R.G. Cooks, Soft landing of ions as a means of surface modification, Int. J. Mass Spectrom. Ion Phys. 23 (1977) 29–35.
[11] B. Gologan, Z. Takáts, J. Alvarez, J.M. Wiseman, N. Talaty, Z. Ouyang, R.G. Cooks, Ion soft-landing into liquids: protein identification, separation, and purification with retention of biological activity, J. Am. Soc. Mass Spectrom. 15 (2004) 1874–1884.
[12] B. Gologan, J.R. Green, J. Alvarez, J. Laskin, R.G. Cooks, Ion/surface reactions and ion soft-landing, Phys. Chem. Chem. Phys. 7 (2005) 1490–1500.
[13] M.A. LaPack, S.J. Pachuta, K.L. Busch, R.G. Cooks, Surface modification by soft landing of reagent beams, Int. J. Mass Spectrom. Ion Phys. 53 (1983) 323–326.
[14] T.A. Blake, Z. Ouyang, J.M. Wiseman, Z. Takáts, A.J. Guymon, S. Kothari, R.G. Cooks, Preparative linear ion trap mass spectrometer for separation and collection of purified proteins and peptides in arrays using ion soft landing, Anal. Chem. 76 (2004) 6293–6305.
[15] M. Volný, W.T. Elam, B.D. Ratner, F. Tureček, Enhanced in-vitro blood compatibility of 316L stainless steel surfaces by reactive landing of hyaluronan ions, J. Biomed. Mater. Res. B Appl. Biomater. 80B (2007) 505–510.
[16] H.J. Räder, A. Rouhanipour, A.M. Talarico, V. Palermo, P. Samorì, K. Müllen, Processing of giant graphene molecules by soft-landing mass spectrometry, Nat. Mater. 5 (2006) 276–280.
[17] U. Heiz, W.-D. Schneider, Size-selected clusters on solid surfaces, Crit. Rev. Solid State Mater. Sci. 26 (2001) 251–290.
[18] S. Vajda, R.E. Winans, J.W. Elam, B. Lee, M.J. Pellin, S. Seifert, G.Y. Tikhonov, N.A. Tomczyk, Supported gold clusters and cluster-based nanomaterials: characterization, stability and growth studies by in situ GISAXS under vacuum conditions and in the presence of hydrogen, Top. Catal. 39 (2006) 161–166.
[19] S. Rauschenbach, F.L. Stadler, E. Lunedei, N. Malinowski, S. Koltsov, G. Costantini, K. Kern, Electrospray ion beam deposition of clusters and biomolecules, Small 2 (2006) 540–547.
[20] H.-P. Cheng, U. Landman, Controlled deposition, soft landing, and glass formation in nanocluster-surface collisions, Science 260 (1993) 1304–1307.
[21] A.M. Bittner, Clusters on soft matter surfaces, Surf. Sci. Rep. 61 (2006) 383–428.
[22] J. Cyriac, T. Pradeep, H. Kang, R. Souda, R.G. Cooks, Low-energy ionic collisions at molecular solids, Chem. Rev. 112 (2012) 5356–5411.
[23] G.E. Johnson, Q. Hu, J. Laskin, Soft landing of complex molecules on surfaces, Annu. Rev. Anal. Chem. 4 (2011) 83–104.
[24] G.E. Johnson, D. Gunaratne, J. Laskin, Soft- and reactive landing of ions onto surfaces: concepts and applications, Mass Spectrom. Rev. 35 (2016) 439–479.
[25] V. Grill, J. Shen, C. Evans, R.G. Cooks, Collisions of ions with surfaces at chemically relevant energies: instrumentation and phenomena, Rev. Sci. Instrum. 72 (2001) 3149–3179.
[26] S.A. Miller, H. Luo, S.J. Pachuta, R.G. Cooks, Soft-landing of polyatomic ions at fluorinated self-assembled monolayer surfaces, Science 275 (1997) 1447–1450.
[27] J. Laskin, G.E. Johnson, J. Warneke, V. Prabhakaran, From isolated ions to multilayer functional materials using ion soft landing, Angew. Chem. Int. Ed. 57 (2018) 16270–16284.
[28] J. Laskin, G.E. Johnson, V. Prabhakaran, Soft landing of complex ions for studies in catalysis and energy storage, J. Phys. Chem. C 120 (2016) 23305–23322.
[29] G. Verbeck, W. Hoffmann, B. Walton, Soft-landing preparative mass spectrometry, Analyst 137 (2012) 4393–4407.
[30] S. Pratihar, G.L. Barnes, J. Laskin, W.L. Hase, Dynamics of protonated peptide ion collisions with organic surfaces: consonance of simulation and experiment, J. Phys. Chem. Lett. 7 (2016) 3142–3150.
[31] M.R. Morris, D.E. Riederer, B.E. Winger, R.G. Cooks, T. Ast, C.E.D. Chidsey, Ion/surface collisions at functionalized self-assembled monolayer surfaces, Int. J. Mass Spectrom. Ion Process. 122 (1992) 181–217.
[32] H. Luo, S.A. Miller, R.G. Cooks, S.J. Pachuta, Soft landing of polyatomic ions for selective modification of fluorinated self-assembled monolayer surfaces, Int. J. Mass Spectrom. Ion Process. 174 (1998) 193–217.
[33] J. Alvarez, R.G. Cooks, S.E. Barlow, D.J. Gaspar, J.H. Futrell, J. Laskin, Preparation and in situ characterization of surfaces using soft landing in a fourier transform ion cyclotron resonance mass spectrometer, Anal. Chem. 77 (2005) 3452–3460.
[34] O. Hadjar, J.H. Futrell, J. Laskin, First observation of charge reduction and desorption kinetics of multiply protonated peptides soft landed onto self-assembled monolayer surfaces, J. Phys. Chem. C 111 (2007) 18220–18225.
[35] O. Hadjar, P. Wang, J.H. Futrell, Y. Dessiaterik, Z. Zhu, J.P. Cowin, M.J. Iedema, J. Laskin, Design and performance of an instrument for soft landing of biomolecular ions on surfaces, Anal. Chem. 79 (2007) 6566–6574.
[36] O. Hadjar, P. Wang, J.H. Futrell, J. Laskin, Effect of the surface on charge reduction and desorption kinetics of soft landed peptide ions, J. Am. Soc. Mass Spectrom. 20 (2009) 901–906.
[37] W.-P. Peng, G.E. Johnson, I.C. Fortmeyer, P. Wang, O. Hadjar, R.G. Cooks, J. Laskin, Redox chemistry in thin layers of organometallic complexes prepared using ion soft landing, Phys. Chem. Chem. Phys. 13 (2010) 267–275.
[38] R. Saf, M. Goriup, T. Steindl, T.E. Hamedinger, D. Sandholzer, G. Hayn, Thin organic films by atmospheric-pressure ion deposition, Nat. Mater. 3 (2004) 323–329.
[39] S. Rauschenbach, R. Vogelgesang, N. Malinowski, J.W. Gerlach, M. Benyoucef, G. Costantini, Z. Deng, N. Thontasen, K. Kern, Electrospray ion beam deposition: soft-landing and fragmentation of functional molecules at solid surfaces, ACS Nano 3 (2009) 2901–2910.
[40] U. Landman, B. Yoon, C. Zhang, U. Heiz, M. Arenz, Factors in gold nanocatalysis: oxidation of CO in the non-scalable size regime, Top. Catal. 44 (2007) 145–158.
[41] W.E. Kaden, T. Wu, W.A. Kunkel, S.L. Anderson, Electronic structure controls reactivity of size-selected Pd clusters adsorbed on TiO_2 surfaces, Science 326 (2009) 826–829.
[42] R.E. Palmer, S. Pratontep, H.-G. Boyen, Nanostructured surfaces from size-selected clusters, Nat. Mater. 2 (2003) 443–448.
[43] V.N. Popok, I. Barke, E.E.B. Campbell, K.-H. Meiwes-Broer, Cluster–surface interaction: from soft landing to implantation, Surf. Sci. Rep. 66 (2011) 347–377.
[44] T.M. Bernhardt, Gas-phase kinetics and catalytic reactions of small silver and gold clusters, Int. J. Mass Spectrom. 243 (2005) 1–29.
[45] J. Lu, L. Cheng, K.C. Lau, E. Tyo, X. Luo, J. Wen, D. Miller, R.S. Assary, H.-H. Wang, P. Redfern, H. Wu, J.-B. Park, Y.-K. Sun, S. Vajda, K. Amine, L.A. Curtiss, Effect of the size-selective silver clusters on lithium peroxide morphology in lithium–oxygen batteries, Nat. Commun. 5 (2014) 4895.
[46] U. Heiz, Size-selected, supported clusters: the interaction of carbon monoxide with nickel clusters, Appl. Phys. A 67 (1998) 621–626.
[47] U. Heiz, A. Sanchez, S. Abbet, W.-D. Schneider, Tuning the oxidation of carbon monoxide using nanoassembled model catalysts, Chem. Phys. 262 (2000) 189–200.
[48] A. Sanchez, S. Abbet, U. Heiz, W.-D. Schneider, H. Häkkinen, R.N. Barnett, U. Landman, When gold is not noble: nanoscale gold catalysts, J. Phys. Chem.A 103 (1999) 9573–9578.
[49] A.S. Wörz, K. Judai, S. Abbet, U. Heiz, Cluster size-dependent mechanisms of the CO + NO reaction on small pdn ($n \leq 30$) clusters on oxide surfaces, J. Am. Chem. Soc. 125 (2003) 7964–7970.
[50] V. Habibpour, C. Yin, G. Kwon, S. Vajda, R.E. Palmer, Catalytic oxidation of cyclohexane by size-selected palladium clusters pinned on graphite, J. Exp. Nanosci. 8 (2013) 993–1003.
[51] Y. Lei, F. Mehmood, S. Lee, J. Greeley, B. Lee, S. Seifert, R.E. Winans, J.W. Elam, R.J. Meyer, P.C. Redfern, D. Teschner, R. Schlögl, M.J. Pellin, L.A. Curtiss, S. Vajda, Increased silver activity for direct propylene epoxidation via subnanometer size effects, Science 328 (2010) 224–228.
[52] S. Lee, L.M. Molina, M.J. López, J.A. Alonso, B. Hammer, B. Lee, S. Seifert, R.E. Winans, J.W. Elam, M.J. Pellin, S. Vajda, Selective propene epoxidation on immobilized Au6–10 clusters: the effect of hydrogen and water on activity and selectivity, Angew. Chem. Int. Ed. 48 (2009) 1467–1471.
[53] S. Abbet, A. Sanchez, U. Heiz, W.-D. Schneider, Tuning the selectivity of acetylene polymerization atom by atom, J. Catal. 198 (2001) 122–127.
[54] S. Lee, M.D. Vece, B. Lee, S. Seifert, R.E. Winans, S. Vajda, Oxidative dehydrogenation of cyclohexene on size selected subnanometer cobalt clusters: improved catalytic performance via evolution of cluster-assembled nanostructures, Phys. Chem. Chem. Phys. 14 (2012) 9336–9342.
[55] C. Fan, T. Wu, W.E. Kaden, S.L. Anderson, Cluster size effects on hydrazine decomposition on Ir_n/Al_2O_3/NiAl(110), Surf. Sci. 600 (2006) 461–467.
[56] M.J. Berr, F.F. Schweinberger, M. Döblinger, K.E. Sanwald, C. Wolff, J. Breimeier, A.S. Crampton, C.J. Ridge, M. Tschurl, U. Heiz, F. Jäckel, J. Feldmann, Size-selected subnanometer cluster catalysts on semiconductor nanocrystal films for atomic scale insight into photocatalysis, Nano Lett. 12 (2012) 5903–5906.
[57] V. Prabhakaran, B.L. Mehdi, J.J. Ditto, M.H. Engelhard, B. Wang, K.D.D. Gunaratne, D.C. Johnson, N.D. Browning, G.E. Johnson, J. Laskin, Rational design of efficient electrode–electrolyte interfaces for solid-state energy storage using ion soft landing, Nat. Commun. 7 (2016), 11399.
[58] A. McInnes, S.R. Plant, I.M. Ornelas, R.E. Palmer, K.G.U. Wijayantha, Enhanced photoelectrochemical water splitting using oxidized mass-selected Ti nanoclusters on metal oxide photoelectrodes, Sustain. Energy Fuels 1 (2017) 336–344.
[59] A.J. Bard, H.D. Abruna, C.E. Chidsey, L.R. Faulkner, S.W. Feldberg, K. Itaya, M. Majda, O. Melroy, R.W. Murray, The electrode/electrolyte interface - a status report, J. Phys. Chem. 97 (1993) 7147–7173.
[60] V. Prabhakaran, G.E. Johnson, B. Wang, J. Laskin, In situ solid-state electrochemistry of mass-selected ions at well-defined electrode–electrolyte interfaces, Proc. Natl. Acad. Sci. 113 (2016) 13324–13329.
[61] Z. Ouyang, Z. Takáts, T.A. Blake, B. Gologan, A.J. Guymon, J.M. Wiseman, J.C. Oliver, V.J. Davisson, R.G. Cooks, Preparing protein microarrays by soft-landing of mass-selected ions, Science 301 (2003) 1351–1354.
[62] E.R. Badman, S. Myung, D.E. Clemmer, Evidence for unfolding and refolding of gas-phase cytochrome c ions in a Paul trap, J. Am. Soc. Mass Spectrom. 16 (2005) 1493–1497.
[63] J.W. McCabe, M. Shirzadeh, T.E. Walker, C.-W. Lin, B.J. Jones, V.H. Wysocki, D.P. Barondeau, D.E. Clemmer, A. Laganowsky, D.H. Russell, Variable-temperature electrospray ionization for temperature-dependent folding/refolding reactions of proteins and ligand binding, Anal. Chem. 93 (2021) 6924–6931.
[64] V.A. Mikhailov, T.H. Mize, J.L.P. Benesch, C.V. Robinson, Mass-selective soft-landing of protein assemblies with controlled landing energies, Anal.

Chem. 86 (2014) 8321–8328.
[65] P. Fremdling, T.K. Esser, B. Saha, A.A. Makarov, K.L. Fort, M. Reinhardt-Szyba, J. Gault, S. Rauschenbach, A preparative mass spectrometer to deposit intact large native protein complexes, ACS Nano 16 (2022) 14443–14455.
[66] M.S. Westphall, K.W. Lee, A.Z. Salome, J.M. Lodge, T. Grant, J.J. Coon, Three-dimensional structure determination of protein complexes using matrix-landing mass spectrometry, Nat. Commun. 13 (2022) 2276.
[67] T.K. Esser, J. Böhning, P. Fremdling, M.T. Agasid, A. Costin, K. Fort, A. Konijnenberg, J.D. Gilbert, A. Bahm, A. Makarov, C.V. Robinson, J.L.P. Benesch, L. Baker, T.A.M. Bharat, J. Gault, S. Rauschenbach, Mass-selective and ice-free electron cryomicroscopy protein sample preparation via native electrospray ion-beam deposition, PNAS Nexus 1 (2022). pgac153.
[68] J.-N. Longchamp, S. Rauschenbach, S. Abb, C. Escher, T. Latychevskaia, K. Kern, H.-W. Fink, Imaging proteins at the single-molecule level, Proc. Natl. Acad. Sci. 114 (2017) 1474–1479.
[69] N. Boisset, P. Penczek, J.-C. Taveau, J. Lamy, J. Frank, J. Lamy, Three-dimensional reconstruction of androctonus australis hemocyanin labeled with a monoclonal fab fragment, J. Struct. Biol. 115 (1995) 16–29.
[70] S.C. Nanita, Z. Takats, R.G. Cooks, S. Myung, D.E. Clemmer, Chiral enrichment of serine via formation, dissociation, and soft-landing of octameric cluster ions, J. Am. Soc. Mass Spectrom. 15 (2004) 1360–1365.
[71] N. Hauptmann, K. Scheil, T.G. Gopakumar, F.L. Otte, C. Schütt, R. Herges, R. Berndt, Surface control of alkyl chain conformations and 2D chiral amplification, J. Am. Chem. Soc. 135 (2013) 8814–8817.
[72] P. Wang, J. Laskin, Helical peptide arrays on self-assembled monolayer surfaces through soft and reactive landing of mass-selected ions, Angew. Chem. Int. Ed. 47 (2008) 6678–6680.
[73] R.R. Hudgins, M.A. Ratner, M.F. Jarrold, Design of helices that are stable in vacuo, J. Am. Chem. Soc. 120 (1998) 12974–12975.
[74] R.R. Hudgins, M.F. Jarrold, Helix Formation in unsolvated alanine-based peptides: helical monomers and helical dimers, J. Am. Chem. Soc. 121 (1999) 3494–3501.
[75] M. Kohtani, T.C. Jones, J.E. Schneider, M.F. Jarrold, Extreme stability of an unsolvated α-helix, J. Am. Chem. Soc. 126 (2004) 7420–7421.
[76] M.F. Jarrold, Helices and sheets in vacuo, Phys. Chem. Chem. Phys. 9 (2007) 1659–1671.
[77] J. Laskin, P. Wang, O. Hadjar, Soft-landing of peptide ions onto self-assembled monolayer surfaces: an overview, Phys. Chem. Chem. Phys. 10 (2008) 1079–1090.
[78] S. Rauschenbach, G. Rinke, N. Malinowski, R.T. Weitz, R. Dinnebier, N. Thontasen, Z. Deng, T. Lutz, P.M. de Almeida Rollo, G. Costantini, L. Harnau, K. Kern, Crystalline inverted membranes grown on surfaces by electrospray ion beam deposition in vacuum, Adv. Mater. 24 (2012) 2761–2767.
[79] Z. Deng, N. Thontasen, N. Malinowski, G. Rinke, L. Harnau, S. Rauschenbach, K. Kern, A close look at proteins: submolecular resolution of two- and three-dimensionally folded cytochrome c at surfaces, Nano Lett. 12 (2012) 2452–2458.
[80] G. Rinke, S. Rauschenbach, L. Harnau, A. Albarghash, M. Pauly, K. Kern, Active conformation control of unfolded proteins by hyperthermal collision with a metal surface, Nano Lett. 14 (2014) 5609–5615.
[81] L. Konermann, D.J. Douglas, Acid-induced unfolding of cytochrome c at different methanol concentrations: electrospray ionization mass spectrometry specifically monitors changes in the tertiary structure, Biochemistry 36 (1997) 12296–12302.
[82] D.E. Clemmer, M.F. Jarrold, Ion mobility measurements and their applications to clusters and biomolecules, J. Mass Spectrom. 32 (1997) 577–592.
[83] C.A. Cassou, H.J. Sterling, A.C. Susa, E.R. Williams, Electrothermal supercharging in mass spectrometry and tandem mass spectrometry of native proteins, Anal. Chem. 85 (2013) 138–146.
[84] J. Ju, Y. Yamagata, T. Higuchi, Thin-film fabrication method for organic light-emitting diodes using electrospray deposition, Adv. Mater. 21 (2009) 4343–4347.
[85] D.J. Carswell, J. Milsted, A new method for the preparation of thin films of radioactive material of thin films of radioactive material, J. Nucl. Energy 4 (1954) 51–54, 1957.
[86] K.F. Lauer, V. Verdingh, Preparation by electro-spraying of thin uranium, plutonium and boron samples for neutron cross section measurements in 4π geometry, Nucl. Instrum. Methods 21 (1963) 161–166.
[87] G.C. Lowenthal, H.A. Wyllie, Special methods of source preparation, Nucl. Instrum. Methods 112 (1973) 353–357.
[88] W. van der Eijk, W. Oldenof, W. Zehner, Preparatio of thin sources, a review, Nucl. Instrum. Methods 112 (1973) 343–351.
[89] C.J. Buchko, K.M. Kozloff, A. Sioshansi, K.S. O'Shea, D.C. Martin, Electric field mediated deposition of bioactive polypeptides on neural prosthetic devices, MRS Online Proc. Libr. 414 (1995) 23–28.
[90] C. Chen, E.M. Kelder, P.J.J.M. van der Put, J. Schoonman, Morphology control of thin LiCoO2 films fabricated using the electrostatic spray deposition (ESD) technique, J. Mater. Chem. 6 (1996) 765–771.
[91] B. Hoyer, G. Sørensen, N. Jensen, D.B. Nielsen, B. Larsen, Electrostatic spraying: a novel technique for preparation of polymer coatings on electrodes, Anal. Chem. 68 (1996) 3840–3844.
[92] T. Thundat, R.J. Warmack, D.P. Allison, T.L. Ferrell, Electrostatic spraying of DNA molecules for investigation by scanning tunneling microscopy, Ultramicroscopy 42–44 (1992) 1083–1087.
[93] V.N. Morozov, T.Ya Morozova, Electrospray deposition as a method for mass fabrication of mono- and multicomponent microarrays of biological and biologically active substances, Anal. Chem. 71 (1999) 3110–3117.
[94] V.N. Morozov, T. Ya, Morozova, electrospray deposition as a method to fabricate functionally active protein films, Anal. Chem. 71 (1999) 1415–1420.
[95] N.V. Avseenko, T.Ya Morozova, F.I. Ataullakhanov, V.N. Morozov, Immobilization of proteins in immunochemical microarrays fabricated by electrospray deposition, Anal. Chem. 73 (2001) 6047–6052.
[96] J. Hou, Q. Zheng, A.K. Badu-Tawiah, C. Xiong, C. Guan, S. Chen, Z. Nie, D. Wang, L. Wan, Electrospray soft-landing for the construction of non-covalent molecular nanostructures using charged droplets under ambient conditions, Chem. Commun. 52 (2016) 13660–13663.
[97] T. He, J.V. Jokerst, Structured micro/nano materials synthesized via electrospray: a review, Biomater. Sci. 8 (2020) 5555–5573.
[98] A. Jaworek, A.T. Sobczyk, Electrospraying route to nanotechnology: an overview, J. Electrost. 66 (2008) 197–219.
[99] A. Jaworek, Electrospray droplet sources for thin film deposition, J. Mater. Sci. 42 (2007) 266–297.
[100] A. Li, Q. Luo, S.-J. Park, R.G. Cooks, Synthesis and catalytic reactions of nanoparticles formed by electrospray ionization of coinage metals, Angew. Chem. Int. Ed. 53 (2014) 3147–3150.
[101] J. Ghosh, R.G. Cooks, Facile synthesis of triazoles using electrospray-deposited copper nanomaterials to catalyze azide-alkyne cycloaddition (AAC) click reactions, ChemPlusChem 87 (2022), e202200252.
[102] D. Sarkar, M.K. Mahitha, A. Som, A. Li, M. Wleklinski, R.G. Cooks, T. Pradeep, Metallic nanobrushes made using ambient droplet sprays, Adv. Mater. 28 (2016) 2223–2228.
[103] J.K. Lee, D. Samanta, H.G. Nam, R.N. Zare, Spontaneous formation of gold nanostructures in aqueous microdroplets, Nat. Commun. 9 (2018) 1562.
[104] D. Sarkar, A. Mahapatra, A. Som, R. Kumar, A. Nagar, A. Baidya, T. Pradeep, Patterned nanobrush nature mimics with unprecedented water-harvesting efficiency, Adv. Mater. Interfac. 5 (2018), 1800667.
[105] S. Bose, A. Chatterjee, S.K. Jenifer, B. Mondal, P. Srikrishnarka, D. Ghosh, A.R. Chowdhuri, M.P. Kannan, S.V. Elchuri, T. Pradeep, Molecular materials through microdroplets: synthesis of protein-protected luminescent clusters of noble metals, ACS Sustain. Chem. Eng. 9 (2021) 4554–4563.
[106] M. Wleklinski, D. Sarkar, A. Hollerbach, T. Pradeep, R. Graham Cooks, Ambient preparation and reactions of gas phase silver cluster cations and anions, Phys. Chem. Chem. Phys. 17 (2015) 18364–18373.
[107] A. Jana, S.K. Jana, D. Sarkar, T. Ahuja, P. Basuri, B. Mondal, S. Bose, J. Ghosh, T. Pradeep, Electrospray deposition-induced ambient phase transition in copper sulphide nanostructures, J. Mater. Chem. A. 7 (2019) 6387–6394.
[108] D. Sarkar, B. Mondal, A. Som, S.J. Ravindran, S.K. Jana, C.K. Manju, T. Pradeep, Holey MoS2 nanosheets with photocatalytic metal rich edges by ambient electrospray deposition for solar water disinfection, Glob. Chall. 2 (2018), 1800052.
[109] D. Sarkar, R. Singh, A. Som, C.K. Manju, M.A. Ganayee, R. Adhikari, T. Pradeep, Electrohydrodynamic assembly of ambient ion-derived nanoparticles to nanosheets at liquid surfaces, J. Phys. Chem. C 122 (2018) 17777–17783.
[110] A.R. Chowdhuri, B.K. Spoorthi, B. Mondal, P. Bose, S. Bose, T. Pradeep, Ambient microdroplet annealing of nanoparticles, Chem. Sci. 12 (2021) 6370–6377.
[111] D. Satyabola, T. Ahuja, S. Bose, B. Mondal, P. Srikrishnarka, M.P. Kannan, B.K. Spoorthi, T. Pradeep, Transformation of nanodiamonds to onion-like carbons by ambient electrospray deposition, J. Phys. Chem. C 125 (2021) 10998–11006.
[112] A. Som, D. Sarkar, S. Kanhirathingal, T. Pradeep, Atomically precise transformations and millimeter-scale patterning of nanoscale assemblies by ambient electrospray deposition, Part. Part. Syst. Char. 34 (2017), 1700101.
[113] A. Fallah-Araghi, K. Meguellati, J.-C. Baret, A.E. Harrak, T. Mangeat, M. Karplus, S. Ladame, C.M. Marques, A.D. Griffiths, Enhanced chemical synthesis at soft interfaces: a universal reaction-adsorption mechanism in microcompartments, Phys. Rev. Lett. 112 (2014), 028301.
[114] S. Narayan, J. Muldoon, M.G. Finn, V.V. Fokin, H.C. Kolb, K.B. Sharpless, "On water": unique reactivity of organic compounds in aqueous suspension, Angew. Chem. Int. Ed. 44 (2005) 3275–3279.
[115] Y. Jung, R.A. Marcus, On the theory of organic catalysis "on water, J. Am. Chem. Soc. 129 (2007) 5492–5502.
[116] N.E. Tarolla, S. Voci, J. Reyes-Morales, A.D. Pendergast, J.E. Dick, Electrodeposition of ligand-free copper nanoparticles from aqueous nanodroplets, J. Mater. Chem. A. 9 (2021) 20048–20057.
[117] H.S. Toh, K. Jurkschat, R.G. Compton, The influence of the capping agent on the oxidation of silver nanoparticles: nano-impacts versus stripping voltammetry, Chem. Eur J. 21 (2015) 2998–3004.
[118] M.W. Glasscott, A.D. Pendergast, J.E. Dick, A universal platform for the electrodeposition of ligand-free metal nanoparticles from a water-in-oil emulsion system, ACS Appl. Nano Mater. 1 (2018) 5702–5711.
[119] A.D. Pendergast, M.W. Glasscott, C. Renault, J.E. Dick, One-step electrodeposition of ligand-free PdPt alloy nanoparticles from water droplets: controlling size, coverage, and elemental stoichiometry, Electrochem. Commun. 98 (2019) 1–5.
[120] Y.E. Jeun, B. Baek, M.W. Lee, H.S. Ahn, Surfactant-free electrochemical synthesis of metallic nanoparticles via stochastic collisions of aqueous nanodroplet reactors, Chem. Commun. 54 (2018) 10052–10055.
[121] A. Li, Z. Baird, S. Bag, D. Sarkar, A. Prabhath, T. Pradeep, R.G. Cooks, Using

ambient ion beams to write nanostructured patterns for surface enhanced Raman spectroscopy, Angew. Chem. Int. Ed. 53 (2014) 12528–12531.
[122] A. Reiser, M. Lindén, P. Rohner, A. Marchand, H. Galinski, A.S. Sologubenko, J.M. Wheeler, R. Zenobi, D. Poulikakos, R. Spolenak, Multi-metal electrohydrodynamic redox 3D printing at the submicron scale, Nat. Commun. 10 (2019) 1853.
[123] V. Jeseentharani, N. Pugazhenthiran, A. Mathew, I. Chakraborty, A. Baksi, J. Ghosh, M. Jash, G.S. Anjusree, T.G. Deepak, A.S. Nair, T. Pradeep, Atomically precise noble metal clusters harvest visible light to produce energy, ChemistrySelect 2 (2017) 1454–1463.
[124] E. Khatun, A. Ghosh, P. Chakraborty, P. Singh, M. Bodiuzzaman, P. Ganesan, G. Nataranjan, J. Ghosh, S. Kumar Pal, T. Pradeep, A thirty-fold photoluminescence enhancement induced by secondary ligands in monolayer protected silver clusters, Nanoscale 10 (2018) 20033–20042.
[125] S. Bag, A. Baksi, S.H. Nandam, D. Wang, X. Ye, J. Ghosh, T. Pradeep, H. Hahn, Nonenzymatic glucose sensing using $Ni_{60}Nb_{40}$ nanoglass, ACS Nano 14 (2020) 5543–5552.
[126] D. Ghosh, M. Bodiuzzaman, A. Som, S. Raja, A. Baksi, A. Ghosh, J. Ghosh, A. Ganesh, P. Samji, S. Mahalingam, D. Karunagaran, T. Pradeep, Internalization of a preformed atomically precise silver cluster in proteins by multistep events and emergence of luminescent counterparts retaining bioactivity, J. Phys. Chem. C 123 (2019) 29408–29417.
[127] H.W. Kroto, J.R. Heath, S.C. O'Brien, R.F. Curl, R.E. Smalley, C_{60}: buckminsterfullerene, Nature 318 (1985) 162–163.
[128] J. Xie, A. Rezvanpour, C.-H. Wang, J. Hua, Electric field controlled electrospray deposition for precise particle pattern and cell pattern formation, AIChE J. 56 (2010) 2607–2621.
[129] A. Yunoki, E. Tsuchiya, Y. Fukui, A. Fujii, T. Maruyama, Preparation of inorganic/organic polymer hybrid microcapsules with high encapsulation efficiency by an electrospray technique, ACS Appl. Mater. Interfaces 6 (2014) 11973–11979.
[130] C. Evans, N. Wade, F. Pepi, G. Strossman, T. Schuerlein, R.G. Cooks, Surface modification and patterning using low-energy ion beams: Si–O bond formation at the vacuum/adsorbate interface, Anal. Chem. 74 (2002) 317–323.
[131] N. Wade, C. Evans, S.-C. Jo, R.G. Cooks, Silylation of an OH-terminated self-assembled monolayer surface through low-energy collisions of ions: a novel route to synthesis and patterning of surfaces, J. Mass Spectrom. 37 (2002) 591–602.
[132] A.K. Badu-Tawiah, C. Wu, R.G. Cooks, Ambient ion soft landing, Anal. Chem. 83 (2011) 2648–2654.
[133] T. Pradeep, B. Feng, T. Ast, J.S. Patrick, R.G. Cooks, S.J. Pachuta, Chemical modification of fluorinated self-assembled monolayer surfaces by low energy reactive ion bombardment, J. Am. Soc. Mass Spectrom. 6 (1995) 187–194.
[134] R.G. Cooks, T. Ast, T. Pradeep, V. Wysocki, Reactions of ions with organic surfaces, Acc. Chem. Res. 27 (1994) 316–323.
[135] D. Tainoff, L. Bardotti, F. Tournus, G. Guiraud, O. Boisron, P. Mélinon, Self-organization of size-selected bare platinum nanoclusters: toward ultra-dense catalytic systems, J. Phys. Chem. C 112 (2008) 6842–6849.
[136] H. Haberland, M. Karrais, M. Mall, A new type of cluster and cluster ion source, Z. Für Phys. At. Mol. Clust. 20 (1991) 413–415.
[137] C. Zhang, H. Tsunoyama, H. Akatsuka, H. Sekiya, T. Nagase, A. Nakajima, Advanced nanocluster ion source based on high-power impulse magnetron sputtering and time-resolved measurements of nanocluster formation, J. Phys. Chem.A 117 (2013) 10211–10217.
[138] M. Shibuta, M. Huber, T. Kamoshida, K. Terasaka, M. Hatanaka, G. Niedner-Schatteburg, A. Nakajima, Size-dependent oxidative stability of silicon nanoclusters mixed with a tantalum atom, J. Phys. Chem. C 126 (2022) 4423–4432.
[139] T. Yokoyama, T. Chiba, N. Hirata, M. Shibuta, A. Nakajima, Electrical conduction of superatom thin films composed of group-V-Metal-Encapsulating silicon-cage nanoclusters, J. Phys. Chem. C 125 (2021) 18420–18428.
[140] H. Tsunoyama, M. Shibuta, M. Nakaya, T. Eguchi, A. Nakajima, Synthesis and characterization of metal-encapsulating Si_{16} cage superatoms, Acc. Chem. Res. 51 (2018) 1735–1745.
[141] H. Tsunoyama, H. Akatsuka, M. Shibuta, T. Iwasa, Y. Mizuhata, N. Tokitoh, A. Nakajima, Development of integrated dry–wet synthesis method for metal encapsulating silicon cage superatoms of $M@Si_{16}$ (M = Ti and Ta), J. Phys. Chem. C 121 (2017) 20507–20516.
[142] M. Shibuta, T. Ohta, M. Nakaya, H. Tsunoyama, T. Eguchi, A. Nakajima, Chemical characterization of an alkali-like superatom consisting of a Ta-encapsulating Si_{16} cage, J. Am. Chem. Soc. 137 (2015) 14015–14018.
[143] M. Nakaya, T. Iwasa, H. Tsunoyama, T. Eguchi, A. Nakajima, Formation of a superatom monolayer using gas-phase-synthesized $Ta@Si_{16}$ nanocluster ions, Nanoscale 6 (2014) 14702–14707.
[144] T. Ohta, M. Shibuta, H. Tsunoyama, T. Eguchi, A. Nakajima, Charge transfer complexation of Ta-encapsulating $Ta@Si_{16}$ superatom with C_{60}, J. Phys. Chem. C 120 (2016) 15265–15271.
[145] M. Shibuta, K. Yamamoto, T. Ohta, T. Inoue, K. Mizoguchi, M. Nakaya, T. Eguchi, A. Nakajima, Confined hot electron relaxation at the molecular heterointerface of the size-selected plasmonic noble metal nanocluster and layered C_{60}, ACS Nano 15 (2021) 1199–1209.
[146] K. Yamagiwa, M. Shibuta, A. Nakajima, Visualization of surface plasmons propagating at the buried organic/metal interface with silver nanocluster sensitizers, ACS Nano 14 (2020) 2044–2052.
[147] C. Zhang, H. Tsunoyama, Y. Feng, A. Nakajima, Extended smoluchowski model for the Formation of size-selected silver nanoclusters generated via modulated pulsed power magnetron sputtering, J. Phys. Chem. C 120 (2016) 5667–5672.
[148] N. Hirata, Y. Katsura, H. Gunji, M. Tona, K. Tsukamoto, M. Eguchi, T. Ando, A. Nakajima, Platinum nanocluster catalysts supported on Marimo carbon via scalable dry deposition synthesis, RSC Adv. 11 (2021) 39216–39222.
[149] K.A. Wepasnick, X. Li, T. Mangler, S. Noessner, C. Wolke, M. Grossmann, G. Gantefoer, D.H. Fairbrother, K.H. Bowen, Surface morphologies of size-selected $Mo_{100\pm2.5}$ and $(MoO_3)_{67\pm1.5}$ clusters soft-landed onto Hopg, J. Phys. Chem. C 115 (2011) 12299–12307.
[150] X. Li, K. Wepasnick, X. Tang, D.H. Fairbrother, K.H. Bowen, A. Dollinger, C.H. Strobel, J. Huber, T. Mangler, Y. Luo, S. Proch, G. Gantefoer, A new nanomaterial synthesized from size-selected, ligand-free metal clusters, J. Appl. Phys. 115 (2014), 104304.
[151] X. Tang, X. Li, Y. Wang, K. Wepasnick, A. Lim, D.H. Fairbrother, K.H. Bowen, T. Mangler, S. Noessner, C. Wolke, M. Grossmann, A. Koop, G. Gantefoer, B. Kiran, A.K. Kandalam, Size selected clusters on surfaces, J. Phys. Conf. Ser. 438 (2013), 012005.
[152] M.A. Denchy, L. Wang, B.R. Bilik, L. Hansen, S. Albornoz, F. Lizano, N. Blando, Z. Hicks, G. Gantefoer, K.H. Bowen, Ultrasmall cluster model for investigating single atom catalysis: dehydrogenation of 1-propanamine by size-selected $Pt_1Zr_2O_7$ clusters supported on Hopg, J. Phys. Chem.A 126 (2022) 7578–7590.
[153] M.A. Denchy, L. Wang, N. Blando, L. Hansen, B.R. Bilik, X. Tang, Z. Hicks, G. Gantefoer, K.H. Bowen, Adsorption and decomposition of dimethyl methylphosphonate on size-selected zirconium oxide trimer clusters, J. Phys. Chem. C 125 (2021) 23688–23698.
[154] X. Tang, D. Bumueller, A. Lim, J. Schneider, U. Heiz, G. Ganteför, D.H. Fairbrother, K.H. Bowen, Catalytic dehydration of 2-propanol by size-selected $(WO_3)_n$ and $(MoO_3)_n$ metal oxide clusters, J. Phys. Chem. C 118 (2014) 29278–29286.
[155] X. Tang, K.H. Bowen, F. Calvo, Self-assembly of $(WO_3)_3$ clusters on a highly oriented pyrolytic graphite surface and nanowire formation: a combined experimental and theoretical study, Phys. Chem. Chem. Phys. 19 (2017) 31168–31176.
[156] B. Kiran, A.K. Kandalam, R. Rallabandi, P. Koirala, X. Li, X. Tang, Y. Wang, H. Fairbrother, G. Gantefoer, K. Bowen, $(PbS)_{32}$: a baby crystal, J. Chem. Phys. 136 (2012), 024317.
[157] A. Dollinger, C.H. Strobel, H. Bleuel, A. Marsteller, G. Gantefoer, D.H. Fairbrother, X. Tang, K.H. Bowen, Y.D. Kim, Growth modes of thin films of ligand-free metal clusters, J. Appl. Phys. 117 (2015), 195302.
[158] P.R. Ellis, C.M. Brown, P.T. Bishop, J. Yin, K. Cooke, W.D. Terry, J. Liu, F. Yin, R.E. Palmer, The cluster beam route to model catalysts and beyond, Faraday Discuss 188 (2016) 39–56.
[159] G.E. Johnson, R. Colby, M. Engelhard, D. Moon, J. Laskin, Soft landing of bare PtRu nanoparticles for electrochemical reduction of oxygen, Nanoscale 7 (2015) 12379–12391.
[160] G.E. Johnson, R. Colby, J. Laskin, Soft landing of bare nanoparticles with controlled size, composition, and morphology, Nanoscale 7 (2015) 3491–3503.
[161] O. Björneholm, M.H. Hansen, A. Hodgson, L.-M. Liu, D.T. Limmer, A. Michaelides, P. Pedevilla, J. Rossmeisl, H. Shen, G. Tocci, E. Tyrode, M.-M. Walz, J. Werner, H. Bluhm, Water at interfaces, Chem. Rev. 116 (2016) 7698–7726.
[162] B.L.V. Prasad, S.I. Stoeva, C.M. Sorensen, K.J. Klabunde, Digestive ripening of thiolated gold nanoparticles: the effect of alkyl chain length, Langmuir 18 (2002) 7515–7520.
[163] J.R. Shimpi, D.S. Sidhaye, B.L.V. Prasad, Digestive ripening: a fine chemical machining process on the nanoscale, Langmuir 33 (2017) 9491–9507.
[164] S. Stoeva, K.J. Klabunde, C.M. Sorensen, I. Dragieva, Gram-scale synthesis of monodisperse gold colloids by the solvated metal atom dispersion method and digestive ripening and their organization into two- and three-dimensional structures, J. Am. Chem. Soc. 124 (2002) 2305–2311.
[165] P. Sahu, B.L.V. Prasad, Time and temperature effects on the digestive ripening of gold nanoparticles: is there a crossover from digestive ripening to ostwald ripening? Langmuir 30 (2014) 10143–10150.
[166] G.E. Johnson, C. Wang, T. Priest, J. Laskin, Monodisperse Au11 clusters prepared by soft landing of mass selected ions, Anal. Chem. 83 (2011) 8069–8072.
[167] G.E. Johnson, T. Moser, M. Engelhard, N.D. Browning, J. Laskin, Fabrication of electrocatalytic Ta nanoparticles by reactive sputtering and ion soft landing, J. Chem. Phys. 145 (2016), 174701.
[168] J. Dong, Y. Wang, Q. Jiang, Z.-A. Nan, F.R. Fan, Z.-Q. Tian, Charged droplet-driven fast formation of nickel–iron (oxy)hydroxides with rich oxygen defects for boosting overall water splitting, J. Mater. Chem. A. 9 (2021) 20058–20067.
[169] J. Ghosh, J. Mendoza, R.G. Cooks, Accelerated and concerted aza-michael addition and SuFEx reaction in microdroplets in unitary and high-throughput formats, Angew. Chem. Int. Ed. n/a (n.d.) e202214090.
[170] K.-H. Huang, J. Ghosh, S. Xu, R.G. Cooks, Late-stage functionalization and characterization of drugs by high-throughput desorption electrospray ionization mass spectrometry, ChemPlusChem 87 (2022), e202100449.
[171] A. Buitrago Santanilla, E.L. Regalado, T. Pereira, M. Shevlin, K. Bateman, L.-C. Campeau, J. Schneeweis, S. Berritt, Z.-C. Shi, P. Nantermet, Y. Liu, R. Helmy,

C.J. Welch, P. Vachal, I.W. Davies, T. Cernak, S.D. Dreher, Nanomole-scale high-throughput chemistry for the synthesis of complex molecules, Science 347 (2015) 49–53.

[172] H. Nie, Z. Wei, L. Qiu, X. Chen, D.T. Holden, R.G. Cooks, High-yield gram-scale organic synthesis using accelerated microdroplet/thin film reactions with solvent recycling, Chem. Sci. 11 (2020) 2356–2361.